European Radiology (2019) 29:2246–2252
https://doi.org/10.1007/s00330-018-5783-6

MAGNETIC RESONANCE

Multicenter validation of the magnetic resonance T2* technique for quantification of pancreatic iron

Antonella Meloni[1] · Daniele De Marchi[1] · Laura Pistoia[1] · Emanuele Grassedonio[2] · Giuseppe Peritore[3] · Paolo Preziosi[4] · Gennaro Restaino[5] · Riccardo Righi[6] · Ada Riva[7] · Stefania Renne[8] · Nicolò Schicchi[9] · Antonino Vallone[10] · Angelo Peluso[11] · Calogera Gerardi[12] · Vincenzo Positano[1] · Alessia Pepe[1]

Received: 20 July 2018 / Revised: 28 August 2018 / Accepted: 20 September 2018 / Published online: 18 October 2018

Abstract

Objectives To assess the transferability of the magnetic resonance imaging (MRI) multislice multiecho T2* technique for pancreatic iron overload assessment.

Methods Multiecho T2* sequences were installed on ten 1.5-T MRI scanners of the three main vendors. Five healthy subjects ($n = 50$) were scanned at each site. Five patients with thalassemia ($n = 45$) were scanned locally at each site and were rescanned at the reference site within 1 month. T2* images were analyzed using a previously validated software and the global pancreatic T2* value was calculated as the mean of T2* values over the head, body, and tail.

Results T2* values of healthy subjects were above 26 ms and showed inter-site homogeneity. The T2* values measured in the MRI sites were comparable to the correspondent values observed in the reference site (12.02 ± 10.20 ms vs 11.98 ± 10.47 ms; $p = 0.808$), and the correlation coefficient was 0.978 ($p < 0.0001$). Coefficients of variation (CoVs) ranged from 4.22 to 9.77%, and the CoV for all the T2* values independently from the sites was 8.55%. The intraclass correlation coefficient (ICC) for each MRI site was always excellent and the global ICC was 0.995, independently from the sites. The mean absolute difference in patients with pancreatic iron ($n = 39$) was -0.15 ± 1.38 ms.

Conclusion The gradient-echo T2* MRI technique is an accurate and reproducible means for the quantification of pancreatic iron and may be transferred among MRI scanners by different vendors in several centers.

Key Points

- *The gradient-echo T2* MRI technique is an accurate and reproducible means for the quantification of pancreatic iron.*
- *The gradient-echo T2* MRI technique for the quantification of pancreatic iron may be transferred among MRI scanners by different vendors in several centers.*
- *Pancreatic iron might serve as an early predictor of cardiac siderosis and is the strongest overall predictor of glucose dysregulation.*

✉ Alessia Pepe
alessia.pepe@ftgm.it

[1] Magnetic Resonance Imaging Unit, Fondazione G. Monasterio CNR-Regione Toscana, Area della Ricerca S. Cataldo, Via Moruzzi, 1 -, 56124 Pisa, Italy

[2] Sezione di Scienze Radiologiche - Dipartimento di Biopatologia e Biotecnologie Mediche, Policlinico "Paolo Giaccone", Palermo, Italy

[3] Unità Operativa Complessa di Radiologia, "ARNAS" Civico, Di Cristina Benfratelli, Palermo, Italy

[4] Unità Operativa Complessa Diagnostica per Immagini, Ospedale "Sandro Pertini", Rome, Italy

[5] Dipartimento di Immagini, Fondazione di Ricerca e Cura "Giovanni Paolo II", Campobasso, Italy

[6] Diagnostica per Immagini e Radiologia Interventistica, Ospedale del Delta, Lagosanto, FE, Italy

[7] Struttura Complessa di Radiologia, Ospedale "SS. Annunziata" ASL Taranto, Taranto, Italy

[8] Struttura Complessa di Cardioradiologia-UTIC, Presidio Ospedaliero "Giovanni Paolo II", Lamezia Terme, Italy

[9] Dipartimento di Radiologia, Azienda Ospedaliero-Universitaria Ospedali Riuniti "Umberto I-Lancisi-Salesi", Ancona, Italy

[10] Reparto di Radiologia, Azienda Ospedaliera "Garibaldi" - Presidio Ospedaliero Nesima, Catania, Italy

[11] Struttura Semplice di Microcitemia, Ospedale "SS. Annunziata" ASL Taranto, Taranto, Italy

[12] Unità Operativa Semplice di Talassemia, Presidio Ospedaliero "Giovanni Paolo II" - Distretto AG2 di Sciacca, Sciacca, AG, Italy

Keywords Magnetic resonance imaging · Pancreas · Iron overload

Abbreviations

CoV	Coefficient of variation
e-MIOT	Extension-Myocardial Iron Overload in Thalassemia
ICC	Intraclass correlation coefficient
LIC	Liver iron concentration
MRI	Magnetic resonance imaging
ROI	Region of interest
SD	Standard deviation
TE	Echo time

Introduction

Iron overload is a serious condition, caused either by increased intestinal iron absorption (e.g., hereditary hemochromatosis) or repeated blood transfusions for hereditary anemias (e.g., thalassemia) or for acquired anemias (e.g., myelodysplastic syndromes or leukemias) [1]. Since the human body has no physiologic mechanism for removing excess iron, chronic transfusions result in accumulation of iron in vital organs [2, 3]. The iron accumulates primarily in the liver and spleen and later on in the endocrine glands and in the heart [4, 5]. Increased iron deposit is cytotoxic and may cause organ dysfunction [6]. Management of iron overload and treatment of iron toxicity by chelation therapy have been demonstrated to reduce iron burden and improve survival [7, 8]. Regular assessment of the iron burden is critical to achieve tailor-made chelation therapies meeting the individual patient's needs [9, 10]. The magnetic resonance imaging (MRI) by the gradient-echo multiecho T2* MRI technique is the most robust method for the noninvasive, sensitive, and fast quantification of organ-specific iron overload [11].

A crucial aspect is the transferability of the T2* technique among different MRI scanners of different manufacturers to expand the availability of high-quality monitoring of iron accumulation to the large cohorts of iron-loaded patients. In fact, it is well known the T2* measurements can be affected by factors dependent from the local magnetic field due technical constraints.

The intra- and inter-operator reproducibility, inter-study reproducibility, and inter-scanner reproducibility of the T2* MRI method for measuring iron concentrations in the heart and liver have already been demonstrated [12–15]. As regards the pancreatic T2*, only the intra- and the inter-operator reproducibility has been assessed in both healthy subjects [16] and TM patients [17]. The intra- and inter-operator reproducibility found in these studies can be considered satisfactory for clinical purposes. However, the transferability of the MRI multislice multiecho T2* technique for pancreatic iron overload assessment has not been evaluated.

Pancreatic iron is a powerful predictor for heart iron and ventricular dysfunction and has a prominent role in the development of abnormal glucose metabolism [5, 18, 19].

The purpose of our study was to assess the transferability of this approach among ten MRI sites by different vendors within the Extension-Myocardial Iron Overload in Thalassemia (e-MIOT) project. e-MIOT is a multicenter, controlled, "no profit" study with the primary aim to validate the T2* sequence for the noninvasive pancreatic iron quantification in patients with hemoglobinopathies.

Materials and methods

Study population

Fifty healthy volunteers (12 females, mean age 36.57 ± 11.51 years), five for each site, including the reference center, were scanned.

Five patients with thalassemia were scanned locally at each site and were rescanned at the reference site in Pisa within 1 month. Mean age of the 45 patients was 37.69 ± 9.31 and 22 (48.9%) were females. Three patients had diabetes mellitus.

The study complied with the Declaration of Helsinki and was approved by the ethical committees of all the sites involved in the study. All subjects gave written informed consent.

MRI

All the subjects underwent MRI using conventional clinical 1.5-T scanners of three main vendors (GE Healthcare, Philips Healthcare, Siemens Healthineers) equipped with eight-element phased-array receiver surface coil. Specifically, the following scanners' sand sites were involved: GE Signa Excite HD (Ancona, Campobasso, Catania, Lamezia, Palermo 1, Palermo 2, Pisa, Roma), Philips Ingenia (Ferrara), and Siemens (Taranto).

To assess the topography of the pancreas, a coronal localizer image was used. Five axial slices covering the abdomen, including the liver and pancreas, were obtained by a T2* gradient-echo multiecho sequence. Each single slice (thickness 8.0 mm) was acquired at ten echo times (first TE 2.0 ms, echo spacing of 2.26 ms) in a single end-expiratory breath hold. The multiecho sequence parameters were as follows: flip angle 25°, matrix 192 × 192 pixels, field of view (FOV) 40 × 40 cm, bandwidth 62.5 KHz, number of excitations 1 [16]. Mean acquisition time was about 3 min.

T2* image analysis was performed using custom-written, previously validated software (HIPPO MIOT®). Three small regions of interest (ROIs) were manually drawn over the head, body, and tail encompassing parenchymal tissue and

taking care to avoid confounding anatomy (e.g., large blood vessels or ducts) and areas involved in susceptibility artifacts from gastric or colic intraluminal gas. For each ROI, the mean value of the signal intensity along all TE values was calculated. The calculated decay curve was fit to a single exponential with a constant offset model. Global pancreatic T2* value was calculated as the mean of T2* values from the three regions. Twenty-six milliseconds was previously demonstrated to be the lowest threshold of normal T2* pancreatic value [16].

All peripheral images were analyzed by a skilled operator (9 years of experience) at the reference center in Pisa, whose intraoperator reproducibility had been previously demonstrated [17].

Cardiac and hepatic T2* values were calculated as previously described [20], and hepatic T2* values were converted into liver iron concentration (LIC) values [21].

Statistical analysis

All data were analyzed using SPSS version 16.0 (SPSS Inc., Chicago, IL, USA) and MedCalc for Windows version 7.2.1.0 (MedCalc Software, Mariakerke, Belgium) statistical packages.

Data were expressed as mean ± standard deviation (SD).

The Kruskal–Wallis test was applied to compare T2* values obtained from MRI images acquired from healthy subjects in different sites.

On patients' T2* values, the measurements of the reference site were assumed correct and the differences in T2* values between scans accounted for a measure of accuracy. Because T2* values were not normally distributed, a paired Wilcoxon signed-rank test was applied to detect significant differences between two datasets while the Spearman correlation coefficient was used to assess their relationship. Summary data were displayed using scatter plots with regression lines. Linear regression models provided the R-squared measuring the goodness of the linear fit. A coefficient of variation (CoV) was calculated as the ratio of the SD of the half mean square of the differences between the repeated values, to the general mean. The intraclass correlation coefficient (ICC) was obtained from a two-way random effects model with measures of absolute agreement. An ICC ≥ 0.75 was considered excellent, between 0.40 and 0.75 good, and < 0.40 unsatisfactory. The Bland–Altman (BA) technique was used to plot the absolute difference (standard BA) or the percent difference (relative BA) versus the average values between two datasets. The relative Bland–Altman plot was preferred when the variability of the differences depended on the magnitude of the measurements. Bias was the mean of the difference between the two methods and agreement was the mean ± 1.96 SDs.

Reproducibility analysis

To evaluate the inter-observer variability, 20 images were presented in random order to an operator of each peripheral center, blinded to the results obtained by the operator in Pisa. Reproducibility was evaluated using CoV, ICC, and Bland–Altman statistics.

Results

Healthy volunteers

On healthy subjects, the global pancreas T2* values ranged from 28.93 to 48.89 ms (mean 37.88 ms, SD 5.08 ms). Table 1 shows the minimum, maximum, and mean global pancreas T2* value for each site. The Kruskal–Wallis test showed no significant difference among the sites ($p = 0.334$).

All T2* values of the three pancreatic regions were above 26 ms, previously demonstrated as the normal T2* pancreatic cutoff [16].

Inter-site reproducibility for thalassemia patients

Twenty-one (46.7%) patients had hepatic iron (MRI LIC > 3 mg/g dw) while 6 (13.3%) patients showed cardiac iron (global heart T2* < 20 ms).

Table 2 shows the global pancreas T2* values measured at the different MRI sites. The global pancreas T2* values ranged from 2.08 to 38.39 ms. The paired Wilcoxon test showed that there was no significant difference between the T2* values measured in the MRI sites and the correspondent values observed in Pisa (12.02 ± 10.20 ms vs 11.98 ± 10.47 ms; $p = 0.808$). All patients categorized as having

Table 1 Global pancreas T2* values of healthy subjects for each MRI site

MRI site	Global pancreas T2* (ms)		
	Minimum	Maximum	Mean ± SD
Pisa	31.31	43.10	38.60 ± 5.40
Ancona	32.53	46.99	40.97 ± 6.05
Campobasso	28.94	42.76	37.34 ± 5.98
Catania	32.92	48.89	38.22 ± 6.40
Ferrara	28.93	40.53	36.34 ± 4.71
Lamezia	34.66	43.45	39.05 ± 4.04
Palermo 1	30.60	40.71	36.22 ± 4.34
Palermo 2	32.64	41.04	37.46 ± 3.45
Roma	35.92	45.06	41.64 ± 4.17
Taranto	28.94	38.28	32.92 ± 4.12

Table 2 Comparison between global pancreas T2* values measured at the different MRI sites and the correspondent values obtained at the reference site

MRI site	Paired Wilcoxon signed-rank test				CoV (%)	ICC
	Reference global pancreas T2* (ms)	Global pancreas T2* at the site (ms)	Mean difference (ms)	*p* value		
Ancona	14.77 ± 10.93	14.2 ± 10.81	0.52 ± 0.79	0.225	4.27	0.998
Campobasso	8.51 ± 2.55	8.45 ± 3.22	0.07 ± 0.88	0.893	6.56	0.981
Catania	6.35 ± 2.78	6.45 ± 2.51	-0.09 ± 0.98	0.893	9.77	0.971
Ferrara	13.72 ± 13.19	12.81 ± 12.04	0.91 ± 1.38	0.138	8.16	0.996
Lamezia	9.02 ± 6.18	9.01 ± 5.73	0.00 ± 0.66	0.686	4.61	0.998
Palermo 1	12.85 ± 9.57	12.80 ± 10.43	0.05 ± 1.81	0.893	8.91	0.993
Palermo 2	22.47 ± 15.65	24.05 ± 12.63	-1.59 ± 3.11	0.225	9.72	0.987
Roma	14.95 ± 14.99	14.98 ± 15.25	-0.03 ± 0.99	0.893	4.22	0.999
Taranto	5.14 ± 3.29	5.37 ± 3.45	-0.22 ± 0.69	0.893	8.86	0.990
All sites	11.98 ± 10.47	12.02 ± 10.20	-0.04 ± 1.47	0.808	8.55	0.995

pancreatic iron overload in the MRI sites, fell in the same category after the MRI executed in Pisa.

There was a strong correlation between the global pancreas T2* values calculated from images obtained in Pisa and at the other MRI sites ($R = 0.978$, $p < 0.0001$).

Figure 1 shows the global pancreas T2* values calculated from images obtained at the nine MRI sites as a function of global pancreas T2* calculated from images obtained in Pisa. The line of best fit had a slope of 0.965 ± 0.021 and an intercept of 0.459 ± 0.328 ms. The R-squared value for the fit was 0.981. Neither constant bias (intercept did not significantly differ from 0) nor proportional bias (angular coefficient did not significantly differ from 1) affected the measurements.

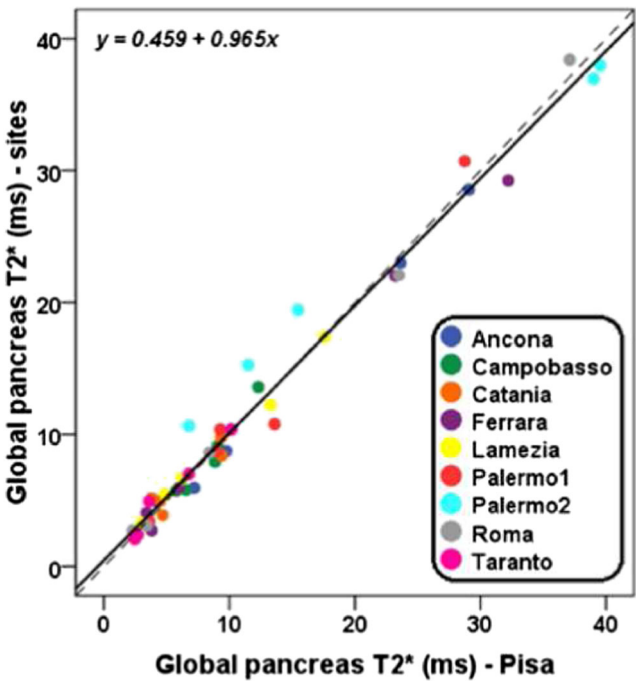

Fig. 1 Scatter plot with regression line showing the relationship between the global pancreas T2* values obtained from images acquired in the nine MRI sites and the correspondent values obtained from images acquired in Pisa. The dotted line represents the unity line

CoVs for all MRI sites are provided in Table 2; they ranged from 4.22 to 9.77%. The CoV for all the T2* values independently from the sites was 8.55%.

The ICC considering all the T2* values, independently from the sites, was 0.995. The ICC for each MRI site is provided in Table 2 and it was always excellent.

The comparison between Pisa and the other MRI sites by Bland–Altman analysis showed a mean absolute difference of -0.04 ± 1.47 ms for the global pancreas T2* values (Fig. 2a). No greater differences for higher T2* values were detected despite the method was developed to better fit lower T2* levels [15]. Three data points, originating only from the Palermo site, were below the 1.96-SD-line. This site was that one with a higher difference, although not significant, when compared to the reference. The relative Bland–Altman (Fig. 2b) showed that the percentage difference increased as the T2* decreased.

The mean absolute difference in patients with pancreatic iron ($n = 39$) was -0.15 ± 1.38 ms.

Table 3 shows the comparison between regional T2* values (head, body, and tail) obtained at the different MRI sites and the reference center. The ICC was always excellent and the CoVs ranged from 4.08 to 14.89%.

Inter-operator reproducibility for thalassemia patients

The results of the inter-observer variability analysis (operator in each MRI site vs operator in Pisa) for global pancreas T2* values are indicated in Table 4. The ICC was excellent and the CoV was < 10% for all operators.

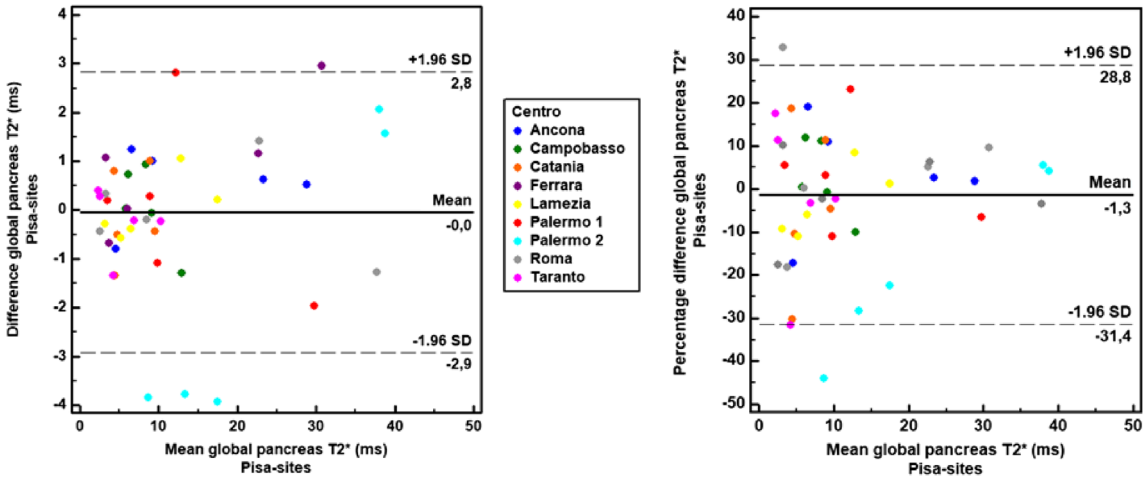

Fig. 2 Absolute (**a**) and relative (**b**) Bland–Altman plots. Dotted lines indicate limits of agreement

Discussion

Pancreatic iron is the strongest overall predictor of glucose dysregulation [19, 22]. Moreover, it is a powerful predictor for heart iron burden and dysfunction [5, 18], providing an early marker of inadequate chelation regimens and a greater time window for intervention.

So, to obtain an accurate and reproducible quantification of pancreatic iron is clinically crucial in iron-loaded patients. Good intra- and inter-observer reproducibility has been shown at the reference site in Pisa [17]. However, for maximal healthcare impact, transferability between scanners of different manufacturers and between sites must be established. This was the purpose of the present study, involving all the MRI sites part of the Italian e-MIOT network [23].

The overall variability depends by different factors: the acquisition phase that involves the scanner and the MRI sequence, the image analysis strategy, and the operator variability. The variability induced by image analysis was canceled since image analysis was performed by the same skilled observer at the reference center in Pisa. We tried to minimize also the variability in the acquisition phase by choosing similar parameters (echo times and sampling bandwidths). Many technical aspects such as the RF coil architecture and shimming algorithms were different, leaving a certain "scan-to-scan" measurement variability. However, the effects of these differences were small, as suggested by previous work on the transferability of the T2* technique for the assessment of iron in other organs [15, 24].

Our data showed that the global pancreas T2* values measured on healthy subjects were comparable among the different sites, indicating full homogeneity.

Correlation, linear regression analysis, CoVs, ICCs, and Bland–Altman analysis for the patient's pancreatic T2* values indicated good agreement and absence of systematic differences between the reference center in Pisa and the other sites. The CoV found for the analysis of pancreatic T2* values was comparable

Table 3 Coefficients of variation, intraclass correlation coefficients, and mean differences for the regional pancreas T2* values measured at the different MRI sites versus the reference site

MRI site	Pancreatic head			Pancreatic body			Pancreatic tail		
	CoV (%)	ICC	Mean diff (ms)	CoV (%)	ICC	Mean diff (ms)	CoV (%)	ICC	Mean diff (ms)
Ancona	9.63	0.992	0.38 ± 2.32	7.75	0.995	-0.22 ± 1.71	5.69	0.997	-0.09 ± 1.25
Campobasso	5.65	0.965	0.18 ± 0.69	13.72	0.913	-0.31 ± 1.70	5.47	0.993	0.34 ± 0.72
Catania	13.58	0.953	-1.08 ± 0.86	13.84	0.929	0.17 ± 1.29	10.32	0.975	0.13 ± 1.04
Ferrara	5.73	0.998	0.63 ± 1.00	14.38	0.989	1.90 ± 2.14	7.79	0.997	0.62 ± 1.44
Lamezia	5.81	0.997	0.51 ± 0.92	12.53	0.986	0.84 ± 1.92	8.32	0.994	-1.02 ± 0.66
Palermo 1	4.08	0.999	0.03 ± 0.90	14.89	0.979	0.90 ± 2.64	14.46	0.981	0.53 ± 2.74
Palermo 2	14.49	0.965	-1.69 ± 5.19	9.46	0.989	-1.78 ± 2.86	8.03	0.992	-1.12 ± 2.54
Roma	7.84	0.997	-0.02 ± 1.87	4.53	0.999	-0.47 ± 0.95	4.40	0.999	0.22 ± 1.00
Taranto	14.74	0.965	-0.13 ± 1.32	14.24	0.982	-0.06 ± 1.11	11.45	0.986	-0.07 ± 0.89
All sites	11.41	0.991	-0.13 ± 2.07	11.71	0.991	0.11 ± 1.99	8.92	0.994	-0.06 ± 1.52

Table 4 Inter-observer reproducibility data

MRI site	CoV (%)	ICC	Bland–Altman bias (ms)	Bland–Altman limits (ms)
Ancona	9.22	0.996	0.43	-2.7 to 2.5
Campobasso	9.99	0.996	0.41	-1.9 to 2.7
Catania	9.51	0.996	0.19	-2.1 to 2.5
Ferrara	7.83	0.997	0.20	-1.7 to 2.1
Lamezia	6.92	0.998	-0.35	-1.9 to 1.3
Palermo 1	8.83	0.997	0.13	-2.1 to 2.3
Palermo 2	9.79	0.996	-0.04	-2.5 to 2.4
Roma	7.39	0.998	-0.14	-2.0 to 1.7
Taranto	7.41	0.998	0.03	-1.8 to 1.9

to that one published for the analysis of cardiac and hepatic T2* values (8.9% and 11.4%, respectively) [15].

In a "real clinical setting," the image analysis is performed by an operator working in the same center where the images are acquired. So, the measurement of reproducibility is affected by the inter-observer variability. To take this into account, 20 images were re-analyzed by an operator of each center. All the peripheral operators obtained T2* values absolutely consistent with those ones calculated by the operator in the reference center (Table 4).

It should be pointed out that, compared to the assessment of cardiac and hepatic iron, the estimate of pancreatic iron is made more complicated by the severe fatty infiltration that can generate a sinusoidal signal fluctuation overimposed to the exponential decay, hampering the goodness of the fit, and the presence of artifacts such as the intraluminal gas in stomach and colon, which in some cases overlap part of the pancreas. In the current work, we used a previously developed and validated approach to deal with these problems: to discard the TEs corresponding to strong deviations from the exponential decay until the fitting error goes below 5% and to follow a conservative method that is to not involve in the T2* analysis pancreatic regions involved in any kind of artifacts or not confidently identifiable on the axial images [16, 17]. Alternatively, conventional fat suppression (FS) techniques can minimize fat signal contributions [17]. However, these techniques are currently not widely available by a single type of fat suppression approach as it occurred in the real world of the e-MIOT network. An effective solution may be the use of fitting models able to separate the R^2* values for fat and water. The hybrid multistep adaptive fitting approach proposed by Zhong et al performed well in both simulated and initial clinical evaluation [25], but, as stated by the authors, still needs further validation.

T2* measurements, in order to quantify iron burden, could be susceptible to other factors such as fibrosis. In a previous study, we showed that myocardial fibrosis did not significantly affect cardiac T2* values [26] and we are confident that the relaxometry should be the same also for the pancreas.

This study has two main limitations. The first limitation is that, due to logistic reasons, we did not assess the inter-study reproducibility. The second limitation is that we did not apply noise-corrected fit methods for the *R2** quantification. However, all the proposed models [27–29] still need further confirming studies and are not generally used in the clinical arena.

In conclusion, the gradient-echo T2* MRI technique is an accurate and reproducible means for the quantification of pancreatic iron and may be transferred among the MRI scanners by different vendors in different centers. The future step will be the calibration of the T2* technique for pancreatic iron quantification against biopsy.

Acknowledgments We thank the patients, who gave their availability for two MRI sessions and long-distance travel within a short time. We also thank the healthy volunteers. We thank C.S. (MRI Lab Secretary) for organization skills.

Funding The authors state that this work has not received any funding.

Compliance with ethical standards

Guarantor The scientific guarantor of this publication is Alessia Pepe.

Conflict of interest The authors of this manuscript declare no relationships with any companies, whose products or services may be related to the subject matter of the article.

Statistics and biometry One of the authors has significant statistical expertise.

Informed consent Written informed consent was obtained from all subjects (patients) in this study.

Ethical approval Institutional Review Board approval was obtained.

Methodology
- Prospective
- Observational
- Multicenter study

References

1. Kremastinos DT, Farmakis D (2011) Iron overload cardiomyopathy in clinical practice. Circulation 124:2253–2263

2. Andrews PA (2000) Disorders of iron metabolism. N Engl J Med 342:1293 author reply 1294
3. Ozment CP, Turi JL (2009) Iron overload following red blood cell transfusion and its impact on disease severity. Biochim Biophys Acta 1790:694–701
4. Maggio A, Capra M, Pepe A et al (2008) A critical review of non invasive procedures for the evaluation of body iron burden in thalassemia major patients. Pediatr Endocrinol Rev 6(Suppl 1):193–203
5. Meloni A, Restaino G, Missere M et al (2015) Pancreatic iron overload by T2* MRI in a large cohort of well treated thalassemia major patients: can it tell us heart iron distribution and function? Am J Hematol 90:E189–E190
6. Hentze MW, Muckenthaler MU, Andrews NC (2004) Balancing acts: molecular control of mammalian iron metabolism. Cell 117:285–297
7. Borgna-Pignatti C, Rugolotto S, De Stefano P et al (2004) Survival and complications in patients with thalassemia major treated with transfusion and deferoxamine. Haematologica 89:1187–1193
8. Pepe A, Meloni A, Rossi G et al (2017) Prediction of cardiac complications for thalassemia major in the widespread cardiac magnetic resonance era: a prospective multicentre study by a multiparametric approach. Eur Heart J Cardiovasc Imaging 19:299–309
9. Argyropoulou MI, Kiortsis DN, Astrakas L, Metafratzi Z, Chalissos N, Efremidis SC (2007) Liver, bone marrow, pancreas and pituitary gland iron overload in young and adult thalassemic patients: a T2 relaxometry study. Eur Radiol 17:3025–3030
10. Pepe A, Meloni A, Rossi G et al (2013) Cardiac and hepatic iron and ejection fraction in thalassemia major: multicentre prospective comparison of combined deferiprone and deferoxamine therapy against deferiprone or deferoxamine monotherapy. J Cardiovasc Magn Reson 15:1
11. Wood JC, Ghugre N (2008) Magnetic resonance imaging assessment of excess iron in thalassemia, sickle cell disease and other iron overload diseases. Hemoglobin 32:85–96
12. Westwood MA, Anderson LJ, Firmin DN et al (2003) Interscanner reproducibility of cardiovascular magnetic resonance T2* measurements of tissue iron in thalassemia. J Magn Reson Imaging 18:616–620
13. Westwood MA, Firmin DN, Gildo M et al (2005) Intercentre reproducibility of magnetic resonance T2* measurements of myocardial iron in thalassaemia. Int J Cardiovasc Imaging 21:531–538
14. Pepe A, Lombardi M, Positano V et al (2006) Evaluation of the efficacy of oral deferiprone in beta-thalassemia major by multislice multiecho T2*. Eur J Haematol 76:183–192
15. Ramazzotti A, Pepe A, Positano V et al (2009) Multicenter validation of the magnetic resonance t2* technique for segmental and global quantification of myocardial iron. J Magn Reson Imaging 30:62–68
16. Restaino G, Meloni A, Positano V et al (2011) Regional and global pancreatic T*(2) MRI for iron overload assessment in a large cohort of healthy subjects: normal values and correlation with age and gender. Magn Reson Med 65:764–769
17. Meloni A, De Marchi D, Positano V et al (2015) Accurate estimate of pancreatic T2* values: how to deal with fat infiltration. Abdom Imaging 40:3129–3136
18. Noetzli LJ, Papudesi J, Coates TD, Wood JC (2009) Pancreatic iron loading predicts cardiac iron loading in thalassemia major. Blood 114:4021–4026
19. de Assis RA, Ribeiro AA, Kay FU et al (2012) Pancreatic iron stores assessed by magnetic resonance imaging (MRI) in beta thalassemic patients. Eur J Radiol 81:1465–1470
20. Meloni A, Restaino G, Borsellino Z et al (2014) Different patterns of myocardial iron distribution by whole-heart T2* magnetic resonance as risk markers for heart complications in thalassemia major. Int J Cardiol 177:1012–1019
21. Meloni A, Rienhoff HY Jr, Jones A, Pepe A, Lombardi M, Wood JC (2013) The use of appropriate calibration curves corrects for systematic differences in liver R2* values measured using different software packages. Br J Haematol 161:888–891
22. Noetzli LJ, Mittelman SD, Watanabe RM, Coates TD, Wood JC (2012) Pancreatic iron and glucose dysregulation in thalassemia major. Am J Hematol 87:155–160
23. Meloni A, Ramazzotti A, Positano V et al (2009) Evaluation of a web-based network for reproducible T2* MRI assessment of iron overload in thalassemia. Int J Med Inform 78:503–512
24. Tanner MA, He T, Westwood MA, Firmin DN, Pennell DJ (2006) Multi-center validation of the transferability of the magnetic resonance T2* technique for the quantification of tissue iron. Haematologica 91:1388–1391
25. Zhong X, Nickel MD, Kannengiesser SA, Dale BM, Kiefer B, Bashir MR (2014) Liver fat quantification using a multi-step adaptive fitting approach with multi-echo GRE imaging. Magn Reson Med 72:1353–1365
26. Meloni A, Pepe A, Positano V et al (2009) Influence of myocardial fibrosis and blood oxygenation on heart T2* values in thalassemia patients. J Magn Reson Imaging 29:832–837
27. Raya JG, Dietrich O, Horng A, Weber J, Reiser MF, Glaser C (2010) T2 measurement in articular cartilage: impact of the fitting method on accuracy and precision at low SNR. Magn Reson Med 63:181–193
28. Feng Y, He T, Gatehouse PD et al (2013) Improved MRI R(2) * relaxometry of iron-loaded liver with noise correction. Magn Reson Med 70:1765–1774
29. Wang C, He T, Liu X, Zhong S, Chen W, Feng Y (2014) Rapid look-up table method for noise-corrected curve fitting in the R2* mapping of iron loaded liver. Magn Reson Med 73:865–871